

Vector soliton fission by reflection at nonlinear interfaces

Fangwei Ye, Yaroslav V. Kartashov, and Lluís Torner

ICFO–Institut de Ciències Fòtoniques, and Universitat Politècnica de Catalunya, Mediterranean Technology Park, 08860 Castelldefels (Barcelona), Spain

Received August 21, 2006; revised October 27, 2006; accepted November 8, 2006; posted November 20, 2006 (Doc. ID 74288); published January 26, 2007

We address the reflection of vector solitons, comprising several components that exhibit multiple field oscillations, at the interface between two nonlinear media. We reveal that reflection causes fission of the input signal into sets of solitons propagating at different angles. We find that the maximum number of solitons that arises upon fission is given by the number of field oscillations in the highest-order input vector soliton.

© 2007 Optical Society of America

OCIS codes: 190.5530, 190.4360, 060.1810.

Spatial vector solitons form when a proper balance between diffraction, self-, and cross-modulation in all light components is achieved.^{1–9} In cubic media, complex vector solitons made of incoherently coupled fields may be stable provided that the strength of cross-modulation coupling does not exceed that of self-modulation. However, strong perturbations modify their internal structure and can lead to their fission. In this Letter we address this phenomenon and reveal that controllable fission does occur by reflection of the vector solitons at the nonlinear interfaces.

The interaction of radiation with nonlinear interfaces gives rise to a number of phenomena, including hysteresis, bistability, and surface wave excitation.^{10–14} Reflection of scalar solitons at nonlinear interfaces has been explored experimentally in Refs. 15–18. Such reflection can cause fission of bound soliton states,¹⁹ a process that motivates this study. Reflection becomes especially complex when several fields are present.^{20,21} We consider reflection of solitons comprising components with multiple field oscillations and find that such a process generates sets of diverging scalar solitons. The maximum number of output solitons is given by the number of field oscillations in the highest-order component and is not equal to the overall number of components, as one might expect.

We address the reflection of vector solitons comprising N mutually incoherent field components at the interface of two cubic media with different refractive indices. The evolution of light beams is described by the system of N coupled nonlinear Schrödinger equations for the dimensionless amplitudes q_n :

$$i \frac{\partial q_n}{\partial \xi} = -\frac{1}{2} \frac{\partial^2 q_n}{\partial \eta^2} - \left[\sum_{k=1}^N |q_k|^2 + H(\eta) \right] q_n. \quad (1)$$

The transverse η and longitudinal ξ coordinates are scaled to the beam width r_0 and the diffraction length $L_{\text{dif}} = kr_0^2$, respectively. The function $H(\eta) = 0$ for $\eta \leq 0$ and $H(\eta) = p$ for $\eta > 0$ describes a refractive index jump at $\eta = 0$. For a beam at wavelength $\lambda = 1.55 \mu\text{m}$ with $r_0 = 10 \mu\text{m}$ propagating in a medium with refractive index $n_0 = 1.5$, $p = 100$ corresponds to a refractive

index step of the order of 10^{-2} ; for a nonlinear coefficient $n_2 \sim 3 \times 10^{-14} \text{ cm}^2/\text{W}$, $q \sim 1$ corresponds to a field intensity $\sim 10^{10} \text{ W/cm}^2$. Such interfaces can be implemented in nematic liquid crystals,¹⁸ or they can be made by stacking together different materials with substantially different refractive indices.¹⁵

In the absence of an interface, vector soliton solutions of Eq. (1) can be found in the form $q_n(\eta, \xi) = w_n(\eta) \exp(ib_n \xi)$. Such solitons contain at least one nodeless component. Components having equal propagation constants $b_k = b_n$ share similar functional shapes. When $b_k \neq b_n$, vector solitons contain components possessing oscillations [see Figs. 1(a) and 1(b) for profiles of two-component solitons]. At $b_2 \rightarrow 0$ the second component vanishes, while at $b_2 \rightarrow b_1$ the soliton transforms into two well-separated vector solitons with two-humped total intensity distribution. In

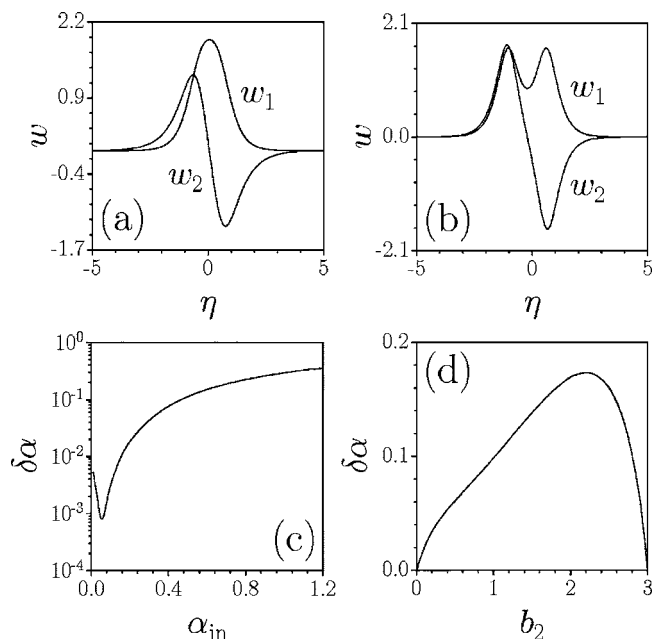


Fig. 1. Profiles of vector solitons at (a) $b_1 = 3$, $b_2 = 1.2$ and (b) $b_1 = 3$, $b_2 = 2.6$. (c) Splitting angle versus incident angle for the vector soliton depicted in panel (a). (d) Splitting angle versus b_2 for the incident angle $\alpha_{\text{in}} = 0.5$ and $b_1 = 3$. In (c) and (d) $p = 100$.

cubic media vector solitons may contain a component with N oscillations only if all lower-order components with $N-1, N-2, \dots$ oscillations are present; thus such solitons include at least N components. The total number of components may exceed N , but then some w_n have similar shapes.

To study the reflection of multicomponent solitons at the interface, we solved Eq. (1) with input conditions $q_n|_{\xi=0} = w_n(\eta + \eta_0)\exp(i\alpha_{\text{in}}\eta)$, where α_{in} is the incident angle, and $\eta_0 \gg 1$ ensures that the soliton is launched far enough from the interface at $\eta=0$. For small incident angles α_{in} the interface reflects solitons almost completely. With increase of α_{in} the amount of radiation penetrating into the region $\eta > 0$ increases so that one may resolve both reflected and transmitted beams in the output pattern. For large enough α_{in} one observes complete soliton refraction. Such behavior occurs for all values of p , but larger p values require greater incident angles for the occurrence of partial and total refraction. Here we are primarily interested in the regime of complete reflection yielding effective vector soliton fission, and we set $p=100$.

The typical dynamics encountered with two-component soliton reflection is shown in Fig. 2. While the fundamental mode keeps its profile and amplitude almost unchanged after reflection, thereby exhibiting quasiparticle behavior, the dipole mode experiences large shape transformations upon reflection. Because of the spatial separation between maxima of the w_2 component, they arrive at the interface at slightly different distances ξ . The right pole of the w_2 component collides with the interface and bounces back in the vicinity of the point $\eta=0$, while the second (left) pole changes its propagation direction in the vicinity of the location where it meets the re-

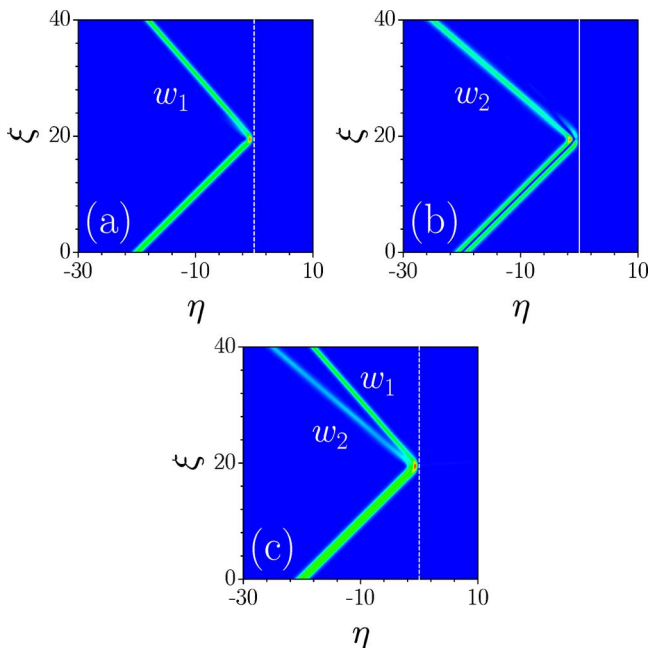


Fig. 2. (Color online) Splitting of two-component vector soliton with $b_1=3$, $b_2=1.2$ into two scalar solitons at $\alpha_{\text{in}}=1$ and $p=100$. Intensities of (a) first and (b) second components; (c) total intensity.

flected right pole and w_1 component. Therefore the left pole of the w_2 component is reflected back at a distance from the interface, in contrast to the w_1 component. This difference in reflection positions leads to different effective potentials experienced by the corresponding fields and yields different reflection angles [Fig. 2(c)]. Notice that upon reflection the energy concentrated in the right hump of the w_2 component couples partially into its left hump, radiative field, and w_1 component, so that the w_2 component loses its dipolelike input structure and reshapes into a single-hump soliton. Thus collision with the interface results in fast fission of input solitons into a set of diverging solitons that are scalar for the chosen set of parameters.

The angle $\delta\alpha$ between two scalar solitons emerging upon reflection versus the incident angle is shown in Fig. 1(c). For the set of parameters in Fig. 1(c) the effective fission of vector soliton occurs at $\alpha_{\text{in}} \lesssim 1.2$, since for larger values of α_{in} refraction dominates. Note that refraction of vector solitons at large incident angles typically does not result in their fission; i.e., rather, vector solitons keep their internal structure after their pass through the interface. At very small angles, $\alpha_{\text{in}} \lesssim 0.01$, the collision is too weak and also does not lead to vector soliton fission. Surprisingly, we found that in the interval $\alpha_{\text{in}} \in [0.01, 1.2]$ the dependence $\delta\alpha(\alpha_{\text{in}})$ is nonmonotonic. The angle $\delta\alpha$ reaches its minimal value at $\alpha_{\text{in}} \approx 0.05$ but never vanishes. At $\alpha_{\text{in}} > 0.05$ the splitting angle increases monotonically. Notice that $\delta\alpha$ is a nonmonotonic function of b_2 as well. The splitting angle vanishes at $b_2 \rightarrow 0$, when the w_2 component goes to zero and may not affect the soliton dynamics, while at $b_2 \rightarrow b_1$, vector solitons transform into two separated and almost independent beams, each of them being reflected at almost equal angles. Thus the most effective fission occurs for intermediate values of b_2 .

We have found similar fission scenarios for higher-order vector solitons containing more than two input components. Fission of the three-component soliton of Fig. 3(a) whose higher-order component possesses three oscillations is depicted in Fig. 3(c). This soliton breaks into three scalar fragments, with the most intensive fragment (in the w_1 component) flying apart at the smallest angle and the less intense fragment (in the w_3 component) flying apart at the largest angle with respect to the ξ axis. Interestingly, one finds that the intensity redistribution inside each component is similar to that for the soliton of Fig. 2: upon reflection, energy concentrated within each component couples into its left outermost hump, which then gives rise to a scalar soliton, while the minimal distance between this hump and the interface increases with the order of the component.

A central result of this Letter is that the number of spatially separated solitons that may emerge upon fission of the vector complexes is determined by the number of oscillations in the highest-order component, and it does not depend on the overall number of components. This point is illustrated in Figs. 3(b) and 3(d), where we show the profile and splitting of a

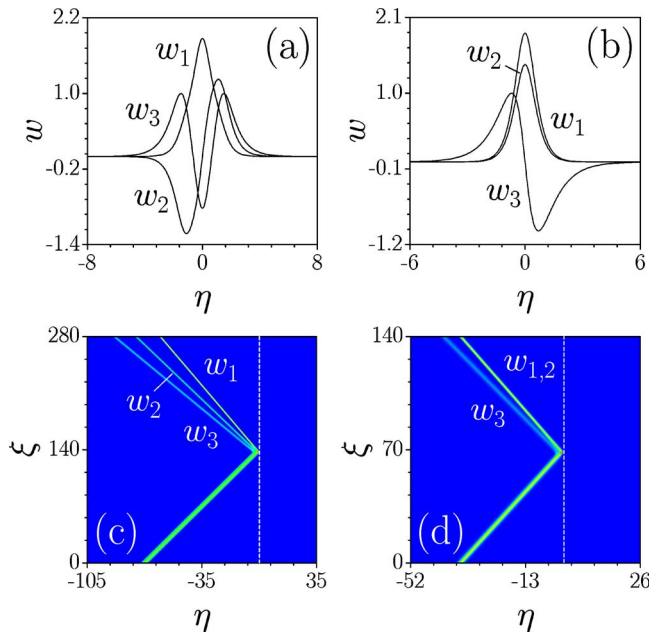


Fig. 3. (Color online) Profiles of three-component vector solitons at (a) $b_1=2.89$, $b_2=1.66$, $b_3=0.86$ and (b) $b_1=3.4$, $b_2=3.4$, $b_3=0.64$. Splitting of solitons from panels (a) and (b) is depicted in panels (c) and (d), correspondingly. In both cases $\alpha_{in}=0.5$ and $p=100$. In (c) and (d) the total intensity distribution is shown.

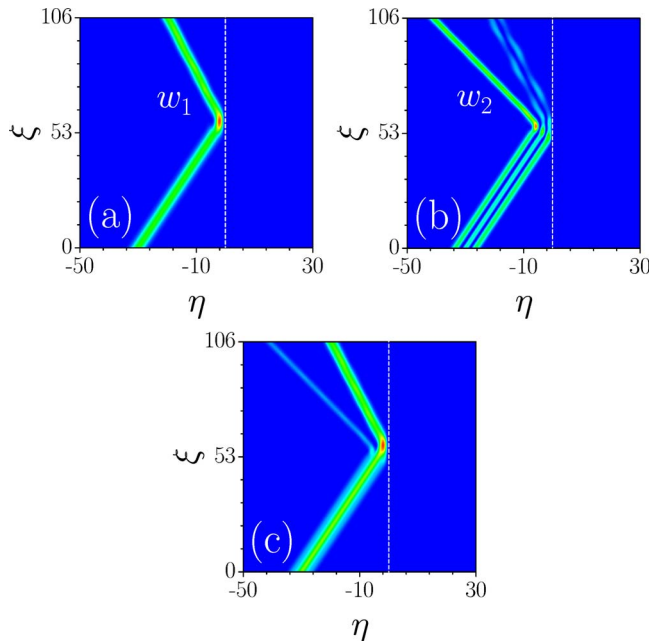


Fig. 4. (Color online) Splitting of a two-component vector soliton with a three-humped second component corresponding to $b_1=1.06$, $b_2=0.66$, at $\alpha_{in}=0.5$ and $p=100$ in a saturable medium with $S=0.8$. (a) First component, (b) second component, (c) total intensity.

three-component soliton for which w_1 and w_2 feature similar shapes. One finds that components possessing similar shapes are always reflected with similar angles irrespective of the energy concentrated within each component. Hence, e.g., in Fig. 3(d) fission of the input vector soliton gives rise to one two-component

vector and one scalar soliton. We checked the validity of this rule by conducting extensive numerical simulations of fission of solitons with as many as 10 components, having different symmetries.

Notice that the results presented here were obtained for the interface of Kerr media and that interfaces between saturable media exhibit different phenomena. Saturable materials support solitons composed of a single nodeless component and components featuring multiple field oscillations, provided that the saturation degree exceeds a critical value.^{7,9} Our numerical simulations showed that reflection of such solitons gives rise to several solitons with different internal structures. For example, reflection of soliton having a nodeless first and a three-humped second component results in the appearance of a scalar soliton and a vector soliton composed of nodeless and dipole components (Fig. 4). The difference from the Kerr case is clearly apparent.

Y. Kartashov's e-mail address is Yaroslav.Kartashov@icfo.es.

References

1. G. I. Stegeman and M. Segev, *Science* **286**, 1518 (1999).
2. S. V. Manakov, *Sov. Phys. JETP* **38**, 248 (1974).
3. J. U. Kang, G. I. Stegeman, J. S. Aitchison, and N. Akhmediev, *Phys. Rev. Lett.* **76**, 3699 (1996).
4. Z. Chen, M. Segev, T. H. Coskun, and D. N. Christodoulides, *Opt. Lett.* **21**, 1436 (1996).
5. D. N. Christodoulides and R. I. Joseph, *Opt. Lett.* **13**, 53 (1988).
6. J. Yang, *Physica D* **108**, 92 (1997).
7. M. Mitchell, M. Segev, and D. N. Christodoulides, *Phys. Rev. Lett.* **80**, 4657 (1998).
8. N. Akhmediev, W. Krolikowski, and A. W. Snyder, *Phys. Rev. Lett.* **81**, 4632 (1998).
9. E. A. Ostrovskaya, Y. S. Kivshar, D. V. Skryabin, and W. J. Firth, *Phys. Rev. Lett.* **83**, 296 (1999).
10. A. E. Kaplan, *JETP Lett.* **24**, 114 (1976).
11. P. W. Smith, J. P. Hermann, W. J. Tomlinson, and P. J. Maloney, *Appl. Phys. Lett.* **35**, 846 (1979).
12. N. N. Akhmediev, V. I. Korneev, and Y. V. Kuzmenko, *Sov. Phys. JETP* **61**, 62 (1985).
13. A. B. Aceves, J. V. Moloney, and A. C. Newell, *Phys. Rev. A* **39**, 1809 (1989).
14. A. B. Aceves, J. V. Moloney, and A. C. Newell, *Phys. Rev. A* **39**, 1828 (1989).
15. E. Alvarado Mendez, R. Rojas Laguna, J. G. Aviña Cervantes, M. Torres Cisneros, J. A. Andrade Lucio, J. C. Pedraza-Ortega, E. A. Kuzin, J. J. Sánchez Mondragón, and V. Vysloukh, *Opt. Commun.* **193**, 267 (2001).
16. L. Jankovic, H. Kim, G. Stegeman, S. Carrasco, L. Torner, and M. Katz, *Opt. Lett.* **28**, 2103 (2003).
17. F. Baronio, C. De Angelis, P.-H. Pioger, V. Couderc, and A. Barthélemy, *Opt. Lett.* **29**, 986 (2004).
18. M. Peccianti, A. Dyadyusha, M. Kaczmarek, and G. Assanto, *Nat. Phys.* **2**, 737 (2006).
19. V. A. Aleshkevich, Y. V. Kartashov, A. S. Zelenina, V. A. Vysloukh, J. P. Torres, and L. Torner, *Opt. Lett.* **29**, 483 (2004).
20. J. Scheuer and M. Orenstein, *Opt. Lett.* **24**, 1735 (1999).
21. I. Shadrivov and A. A. Zharov, *Opt. Commun.* **216**, 47 (2003).